

Radiation Environment in Concrete Biological Shields of Nuclear Power Plants

Igor Remec
Oak Ridge National Laboratory

1. Introduction

Since 2000, numerous nuclear power plants (NPPs), which were originally licensed and designed to operate 40 years, have undergone a license renewal process to extend their permission to operate up to 60 years. Moreover, additional life extensions to 80 or even 100 years are under consideration. In order to insure safe operation of NPPs throughout their longer lifetimes, understanding and predicting long-term degradation of materials is necessary. And although the effects of irradiation on reactor pressure vessels (RPVs) are monitored by extensive surveillance programs throughout their operational lives, the effects of irradiation on concrete structures has not undergone similar evaluation.

Existing irradiated concrete data, based mostly on data compiled by Hilsdorf [1], suggests that some radiation-induced degradation of concrete may appear at neutron fluence above 1.0×10^{19} neutrons/cm² and / or gamma dose above 1.0×10^{10} rads. There is, however, little known about the details of experiments reported in [1], such as the concrete composition and temperature, neutron spectrum, and the effects of simultaneous neutron and gamma-ray irradiation. Therefore, there is a need to improve and expand the database on irradiated concrete degradation and develop an understanding of the basic mechanisms causing radiation damage.

Pressurized water reactors (PWRs) typically exhibit higher radiation levels outside the PV than the boiling water reactors. Among the PWRs, the highest radiation levels outside the PVs are typically observed at two-loop plants, followed by lower levels at three-loop plants and at the lowest levels at four-loop plants.

In the present work we discuss neutron and gamma fields in the concrete biological shield of a selected 3-loop and 2-loop pressurized water reactors (PWR). Some of the basic characteristics of the two plants considered are listed in Table 1. Results of radiation transport simulations are presented and discussed.

2. Assessment of Radiation Fields and Discussion

In this section, interesting aspects of the neutron and gamma fields will be described without attempting to provide a comprehensive discussion of the subject.

The variation of the neutron and gamma-ray flux with the radial distance from the core center, through the PV, cavity and concrete shield is shown in Fig. 1 for the 3-loop plant and Fig. 2 for the 2-loop plant. The shapes of the flux distributions for the 2-loop and 3-loop plants are quite similar. Neutron fluxes for all energies, except the thermal neutron flux, exhibit a monotonic decrease through the PV, cavity and inside

the concrete shield. However, the rate of attenuation varies depending on the material. For example, it is large in the RPV steel and in the biological shield concrete but very small through the air in the cavity region. Gamma-ray flux shows similar behavior. However, thermal neutron flux ($E < 0.41$ eV), behaves remarkably different: the ‘U’ shape in the PV wall indicates that thermal neutrons penetrate into the wall from both surfaces, due to the higher thermal flux levels in the water coolant inside the PV and air and concrete outside the PV. From the outer wall, thermal flux increases in the outward direction and reaches local maximum about 8 -10 cm (3”-4”) inside concrete wall. The local flux maximum inside concrete wall is caused by strong down-scattering of higher energy neutrons in concrete.

Figs. 3 and 4 show radial variation of neutron and gamma-ray flux and neutron and gamma heating rates for the 3-loop and 2-loop PWRs. The neutron and gamma heating rates follow the general trends for the neutron and gamma flux within each material zone; however, the neutron heating rate in air is sharply higher than in steel due to the presence of lighter elements in the air. This causes a steep increase in neutron heating rate at the transition from the PV to the cavity.

The model of the 3-loop plant included ~ 100-cm thick concrete shield and ex-vessel neutron detector wells while concrete thickness in the 2-loop plant model was only ~ 16 cm and no detector wells were included. This caused faster attenuation of fluxes in the 2-loop plant concrete shield, which can be seen from the comparison of Figs. 1 and 2 and Figs. 3 and 4. At this point we were primarily concerned with the radiation fields close to the inner surface of the concrete; however, a thicker shield may be considered at a later time.

Figs. 5 and 6 depict the azimuthal variation of the neutron and gamma flux just inside the biological shield. For the 3-loop plant, which included the ex-vessel detector cavities in the model, approximately 8-degrees of the arc close to the 0-degrees and 45-degrees azimuth are in the air. This causes the change in shape in the azimuthal distribution in the 3-loop plant as compared to smooth distribution shown for the 2-loop plant. The 2-loop plant also has ex-vessel detector wells, but they were not included in the model in order to show the effect on the radiation fields and heating rates. The importance of the ex-vessel cavities is further illustrated in Figs. 7 and 8, which depict azimuthal variation of neutron and gamma heating rates for the 3-loop and 2-loop PWR. There is a significant drop in neutron heating rate where the material changes from air to concrete for the 3-loop PWR. Based on Figs. 7 and 8, it appears reasonable to suggest that in the presence of ex-vessel detector wells, the highest heating rate in concrete will appear at a location that is closest to – but not coincident with – the highest fast neutron flux location. In the absence of detector wells the peak locations of fluxes and heating rates coincide (Fig. 8).

The variation of radiation fields with elevation is small in the wide region close to the core mid-plane. For example, Fig. 9 shows the fast neutron flux ($E > 1$ MeV) versus elevation for the 2-loop PWR, where the fast flux is shown at the location of its maximum in the concrete shield (at $\theta = 0$ degrees). The distribution for the 3-loop plant is similar and is not shown here.

Neutron and gamma-ray spectra in the cavity region of the 3-loop and 2-loop PWR are quite similar, as demonstrated in Figs. 10 and 11.

Finally, the variation of the total-to-fast flux ($E > 1$ MeV)-ratio in the radial direction from the inner wall of the PV, through the cavity and inside the concrete shield is shown in Figs. 12 and 13 for a 3-loop PWR and 2-loop PWR. Large variations can be seen. For the 3-loop PWR, the large impact of the detector well

is observed at 8-degrees of arc , as was previously noted. The thermal neutron flux at any given location depends to a large extent on the moderating properties of the local material and does not necessarily follow the distribution of the higher energy neutrons. Figs. 12 and 13 are shown in order to emphasize that without knowing the details of experiments, such as those reported in [1], it is practically impossible to renormalize result from fast neutron fluence ($E > 1\text{MeV}$) to total neutron fluence or vice versa.

Table 2 summarizes the neutron fluxes, gamma-ray fluxes and neutron and gamma-ray heating rates at the PV outer radius and at the point of maximum heating in concrete, for the 2-loop and 3-loop plant. The 2-loop plant analyzed has 2-4 times higher neutron and gamma fluxes and heating than the 3-loop plant considered. A similar analysis was performed by TransWare [2] on a 3-loop plant. Their results indicate similar trends as described in this report.

Table 3 provides an estimate of the years of operation to accumulate neutron fluence of $1 \times 10^{19} \text{ cm}^{-2}$, $5 \times 10^{19} \text{ cm}^{-2}$, and $1 \times 10^{20} \text{ cm}^{-2}$, and gamma-ray dose of 1×10^{10} rads, for the 2-loop and 3-loop plant, based on fluxes in concrete which are listed in Table 2. Besides total neutron fluence ($E > 0 \text{ eV}$), neutron fluences above 0.1 MeV and 1 MeV are considered. For gamma-ray fluence, the energy threshold is 0.01 MeV. Both the 2-loop and 3-loop plants reach the $1 \times 10^{19} \text{ cm}^{-2}$ total neutron fluence in concrete early in their lives, namely after 5 and 11 years. The 2-loop plant also exceeds the $1 \times 10^{20} \text{ cm}^{-2}$ total neutron fluence level after 55 years of operation. Neither of the two plants would reach the $1 \times 10^{19} \text{ cm}^{-2}$ fast ($E > 1 \text{ MeV}$) neutron fluence within 100 years of operation. The 2-loop plant is projected to reach a gamma-ray dose of 1×10^{10} rad in 70 years, while the 3-loop plant will stay below this threshold even for 100 years of operation.

Due to the paucity of irradiated concrete data at high fluence [1], concrete irradiation experiments with irradiation times limited to 1 to 2 years have been considered. Moreover, Japanese experiments [3] are planned to begin in 2013 at the JEEP II reactor at Kjeller, Norway. To accumulate neutron and gamma fluences equivalent to a PWR operated for 100 years, an acceleration factor of 50 to 100 is necessary. Table 4 lists neutron and gamma-ray fluxes and heating rates, based on Table 2 values for 2-loop PWR in concrete, for acceleration factors of 50 and 100. It is noted that the heating rates for accelerated irradiation are quite high, in the range from 4.3 to 8.6 W/kg.

3. Summary Observation and Comments

Based on the comparisons presented in section 2 and the summary of observations from the calculations performed for the 3-loop and 2-loop PWR listed in Table 2, one can observe that:

- 1) Fast neutron ($E > 1\text{MeV}$ and $E > 0.1\text{ MeV}$) fluxes at the pressure vessel (PV) outer radius are 20-30% higher than the maximum fluxes in concrete. These fluxes, determined at the maximum at the PV wall, are typically provided in reactor pressure vessel surveillance reports. These values could be used as conservative estimates for the fluxes in the concrete shield or for screening purposes.

The total neutron flux is 0 - 10% higher and gamma flux is 2% lower to 5% higher at the PV outer wall compared to the maximum value in concrete.

The exception is thermal neutron flux, which is 50-100% higher in the concrete. Thermal flux is subject to large local variations depending on the local material.

Heating rates calculated at the PV maximum flux location are also 10-20% higher than the highest rates in concrete.

Based on results shown in Figs. 12 and 13, it is practically impossible to renormalize result from fast neutron fluence ($E > 1\text{MeV}$) to total neutron fluence or vice versa without knowing the details of the irradiation experiment.

- 2) Azimuthal variations in fluxes, due primarily to the specific layout of the core-PV-biological-shield regions, are pronounced. Therefore, if cavity dosimetry results are to be used to estimate maximum fluxes in the biological shield and the azimuthal locations of the two positions are significantly different, corrections based on azimuthal distribution will likely be necessary. On the other hand, since variations in vertical direction are relatively small and if dosimetry is in the core beltline region, the results should not require corrections for vertical position.

For determination of maximum PV flux locations, the concrete shield shape (e.g. location of ex-core detector cavities) needs to be taken into account. A simple rule appears to be that the maximum heating rate and maximum fluxes in concrete will be in the concrete closest to the location of maximum flux on the PV outer wall.

- 3) 2-loop and 3-loop PWRs have quite similar neutron and gamma-ray spectra in the cavity region.
- 4) The 2-loop plant analyzed has 2-4 times higher neutron and gamma fluxes and heating than the 3-loop plant considered. The 4-loop plants are expected to have lower fluxes outside the PV; however, this needs to be confirmed. Since both plants analyzed in this report were designed by Westinghouse, additional work will be required for different designs.

With regard to preparation of concrete irradiation experiments, the following comments and suggestions can be offered:

- 1) Since the relevant irradiation parameters for concrete have not been established, it is desirable to obtain full neutron and gamma spectra in the samples for the experiments.
- 2) Irradiation experiments should be designed so that the neutron and gamma spectra in the concrete samples will be similar to those observed in NPPs biological shields.
- 3) Accelerated irradiation experiments will require considerably higher neutron and gamma fluxes than those observed in the shields on NPPs. The acceleration factor, and therefore fluxes are anticipated to be higher by a factor of 50-100. Analysis of the temperature of the samples will be necessary and additional cooling of concrete samples may be needed.

4. References

[1] H. Hilsdorf, J. Kropp, H. Kock, "The Effects of Nuclear Radiation on the Mechanical Properties Of Concrete," American Concrete Institute Report SP-55-10, 1978.

[2] "An Evaluation of Neutron, Gamma, and Temperature Profiles in a Three-Lopp PWR Biological Shield," TWE-LPI1-001-R-001, Feb. 19, 2013

[3] I. Maruyama, O. Kontani, A. Ishizawa, M. Takizawa, O. Sato, "Development of System for Evaluating Concrete Strength Deterioration Due to Radiation and Resultant Heat," IAEA-CN-194-093, Proceedings of the IAEA, International Conference on Plant Life Management, 2012, Salt Lake City, UT, May 13-17, 2012.

Table 1. Some properties of the selected PWRs.

Plant	TYPE	Thermal Power	PV Thickness	Thickness of Reactor Cavity	Inner Radius of Biological Shield
Plant A	3-loop PWR (W) HBR-2	2300 MW	24.17 cm (9.5 “)	17.1 cm (6.7”)	238.76 cm (7’ 10”)
Plant B	2-loop PWR (W) Krsko	1876 MW	16.84 cm (6.6”)	16 cm (6.3”)	200.6 cm (6’ 7”)

Table 2. Summary and comparison of neutron and gamma fluxes and heating rates in 3-loop and 2-loop PWR.

	Neutron Flux				Gamma Flux	Heating Rate ^a		
	E > 1MeV	E > 0.1 MeV	E < 0.41 eV	E > 0 eV	E > 0.01 MeV	Gamma	Neutron	N + G
	(cm ⁻² s ⁻¹)				(cm ⁻² s ⁻¹)	(rad/s)		
2-loop PWR								
At PV OR at Maximum	3.58E+09	3.04E+10	3.06E+09	6.77E+10	9.53E+09	5.87	4.70	10.57
In Concrete at Maximum	2.79E+09	2.41E+10	4.64E+09	6.29E+10	9.08E+09	4.90	3.70	8.60
Ratio	0.78	0.79	1.52	0.93	0.95	0.83	0.79	0.81
3-loop PWR								
At PV OR at Maximum	1.04E+09	1.43E+10	1.08E+09	3.09E+10	3.29E+09	2.15	2.06	4.20
In Concrete at Max. Heating Rate	7.49E+08	1.13E+10	2.24E+09	3.10E+10	3.37E+09	2.00	1.60	3.60
Ratio	0.72	0.79	2.08	1.00	1.02	0.93	0.78	0.86
Ratio 2-loop/3-loop								
At PV OR at Maximum	3.45	2.12	2.84	2.19	2.90	2.73	2.29	2.51
In Conc., at Max. Heating Rate	3.72	2.13	2.07	2.03	2.69	2.45	2.31	2.39

^aHeating rates at PV outer radius are calculated with flux-to-dose conversion factors for concrete even though the actual material at that location is air. This was done to allow easier comparison with heating rates in biological shield.

Table 3. Years of operation to reach neutron fluence of $1 \times 10^{19} \text{ cm}^{-2}$, $5 \times 10^{19} \text{ cm}^{-2}$, and $1 \times 10^{20} \text{ cm}^{-2}$ and gamma-ray dose of 1×10^{10} rads. Three different energy thresholds for neutron fluence are considered. A 92% load (efficiency) factor is assumed for the plant operation.

Calendar Years of Operation to Reach Selected Neutron Fluence and Gamma-Ray Dose Rate Levels					
Fluence or Dose	NPP Type	Neutron Flux Energy Threshold			Gamma-Rays
		E > 0 eV	E > 0.1 MeV	E > 1MeV	E > 0.01MeV
Fluence $1 \times 10^{19} \text{ cm}^{-2}$	2-loop	5	14	123	
	3-loop	11	30		
Fluence $5 \times 10^{19} \text{ cm}^{-2}$	2-loop	27	71		
	3-loop	56	152		
Fluence $1 \times 10^{20} \text{ cm}^{-2}$	2-loop	55	143		
	3-loop	111			
Gamma-Ray Dose 1×10^{10} rad	2-loop				70
	3-loop				172

Table 4 Estimated fluxes for concrete irradiation experiment for the 50- and 100-times acceleration factor, based on 2-loop PWR values in concrete from Table 2. Accumulated fluences and doses are also given.

	Neutron Flux ($\text{cm}^{-2} \text{ s}^{-1}$)				Gamma Flux ($\text{cm}^{-2} \text{ s}^{-1}$)	Heating Rate (rad/s)		
	E > 1MeV	E > 0.1 MeV	E < 0.41 eV	E > 0 eV	E > 0.01 MeV	Gamma	Neutron	N + G
Acceleration Factor 50 (2-year irradiation)	1.40 E+11	1.21 E+12	2.32 E+11	3.15E+12	4.54E+11	245	185	430
Acceleration factor 100 (1 year irradiation)	2.79 E+11	2.41E+12	4.64E+11	6.29E+12	9.08 E+11	490	370	860
	Neutron Fluence (cm^{-2})				Gamma Fluence (cm^{-2})	Accumulated Dose (rad)		
						Gamma	Neutron	N + G
2-year Irradiation, at 50 x Acceleration Or 1-year Irradiation, at 100 x Acceleration	8.84 E+18	7.61E+19	1.46E+19	1.99E+20	2.87E+19	1.55 E+10	1.17E+10	2.71E+10

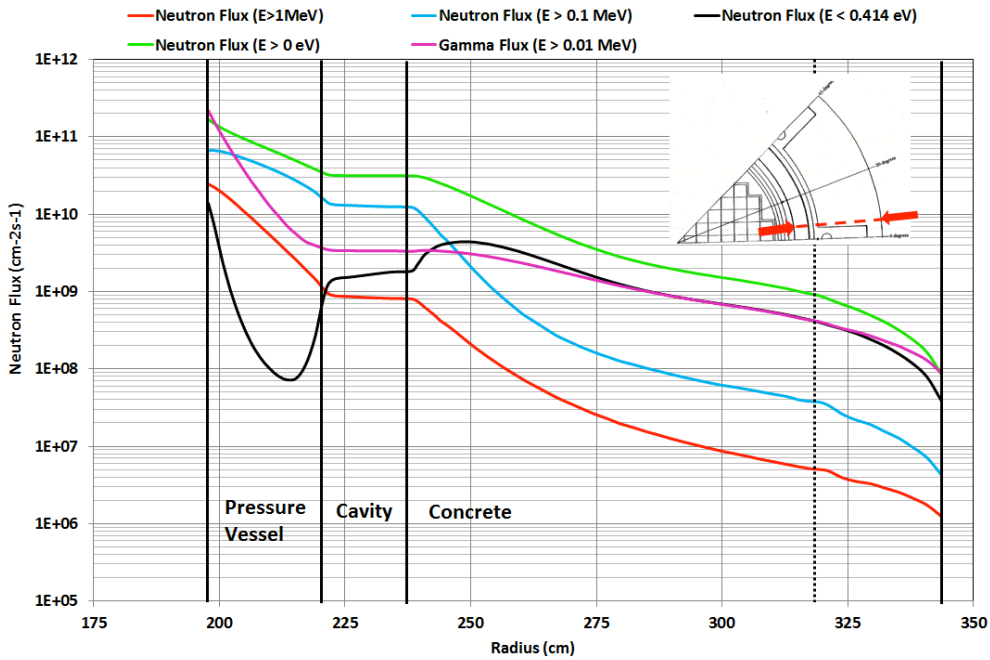


Fig. 1 Neutron and gamma-ray flux versus distance from the core for the 3-loop PWR plant. The insert shows the location of the radial segment plotted on the ordinate. Different curves depict fluxes with energies above the threshold energy given in the parenthesis. The dotted vertical line at the right side marks the outer edge of the detector well.

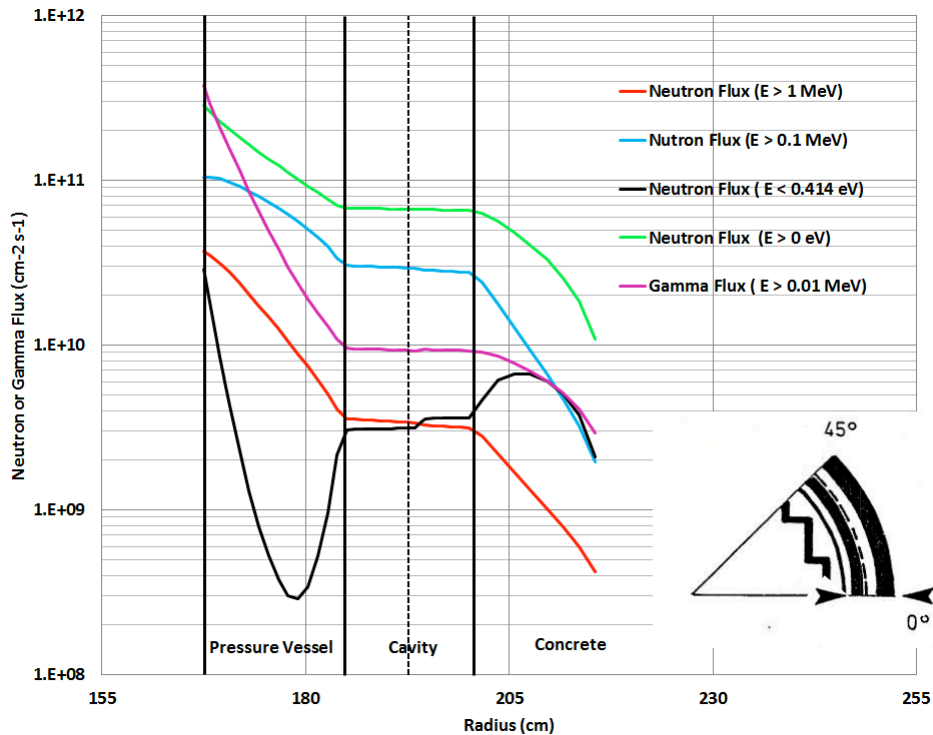


Fig. 2 Neutron and gamma-ray flux versus distance from the core for the 2-loop PWR plant. The insert shows the location of the radial segment plotted on the ordinate. Different curves depict fluxes with energies above the threshold energy given in the parenthesis. The dashed vertical line in the cavity marks the outer edge of thermal isolation.

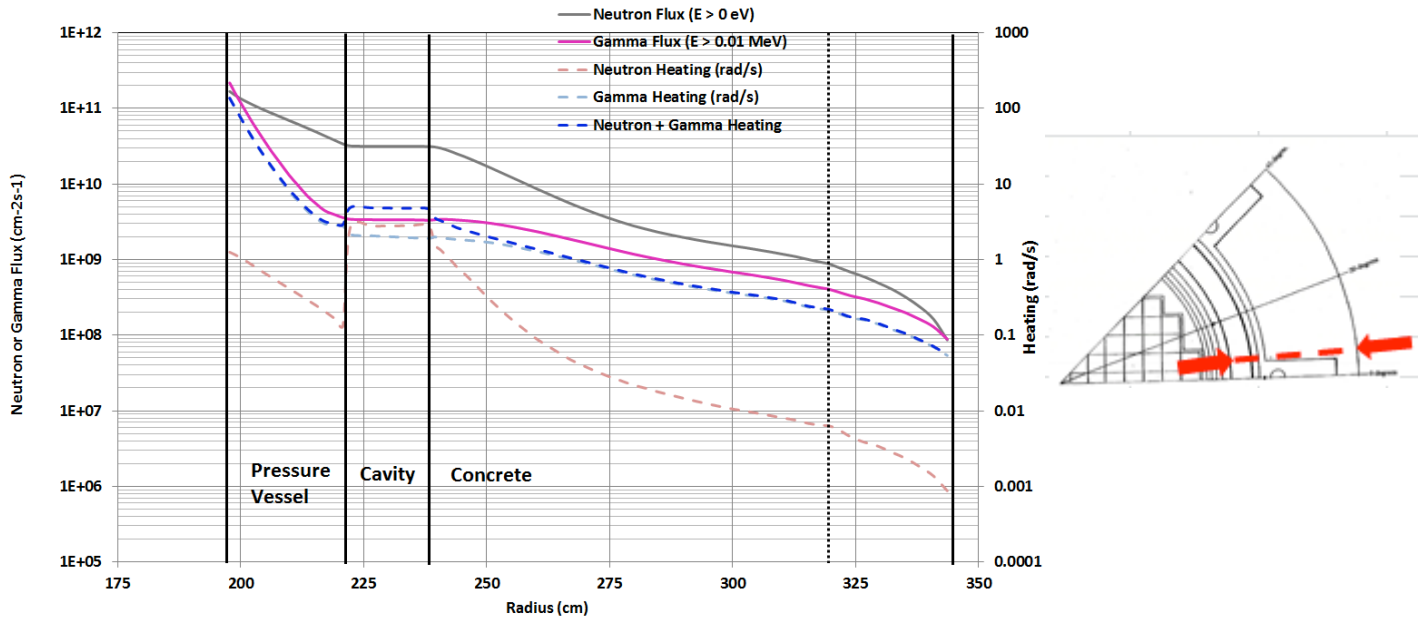


Fig. 3 Radial variation of neutron and gamma-ray flux and heating rates for a 3-loop PWR. Radial variation is shown at approximately the position of maximum heating rate in concrete.

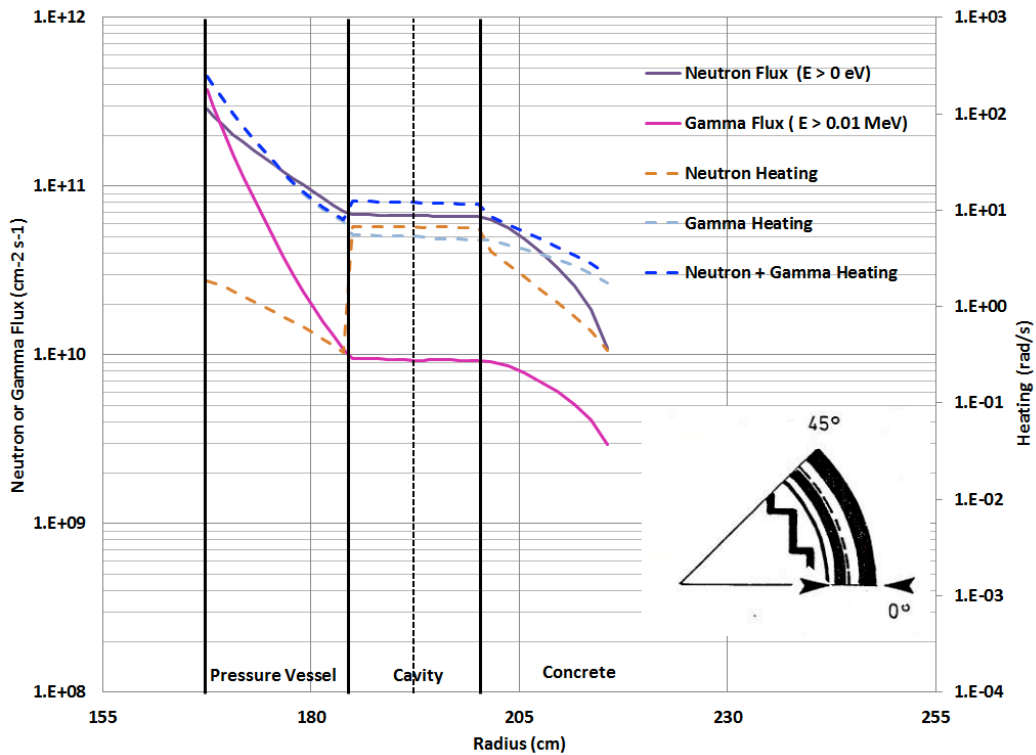


Fig. 4 Radial variation of neutron and gamma-ray flux and heating rates for a 2-loop PWR.

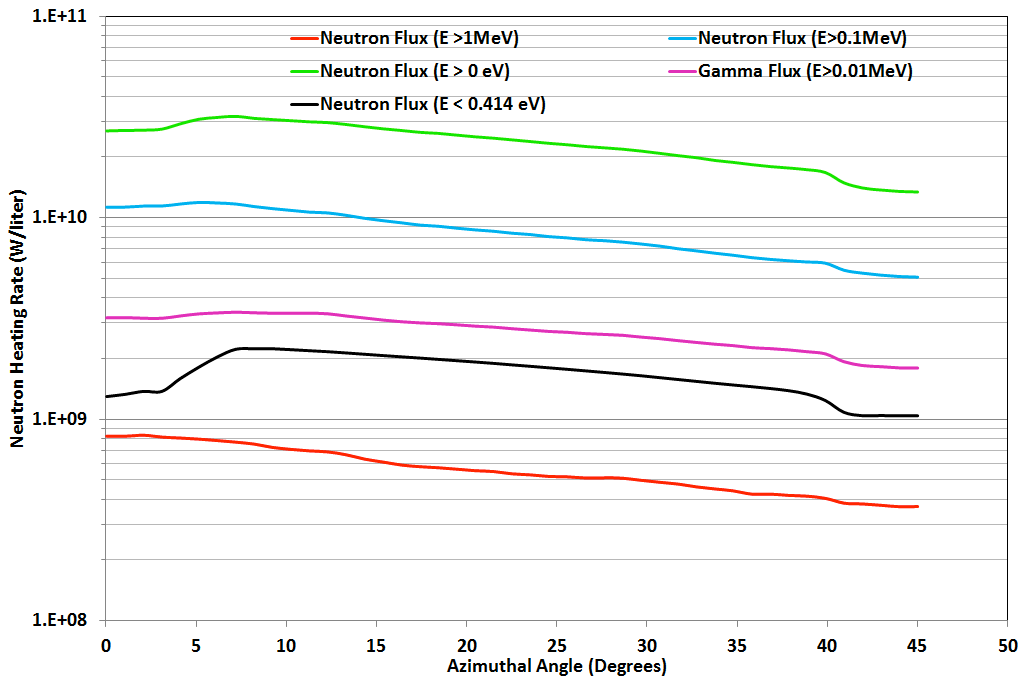


Fig. 5 Azimuthal variation of neutron and gamma flux along the radial arc just inside the cylindrical part of the biological shield (as shown in the insert at the right side) for a 3-loop PWR.

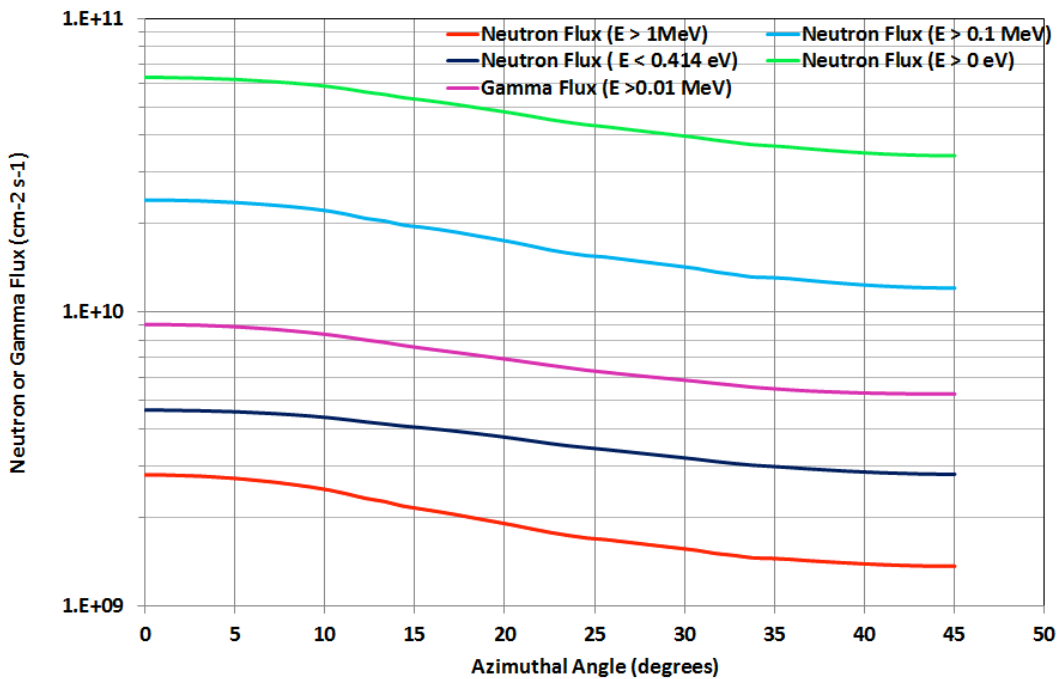


Fig. 6 Azimuthal variation of neutron and gamma flux along the radial arc just inside the biological shield (as shown in the insert at the right side) for a 2-loop PWR (without the ex-vessel detector well).

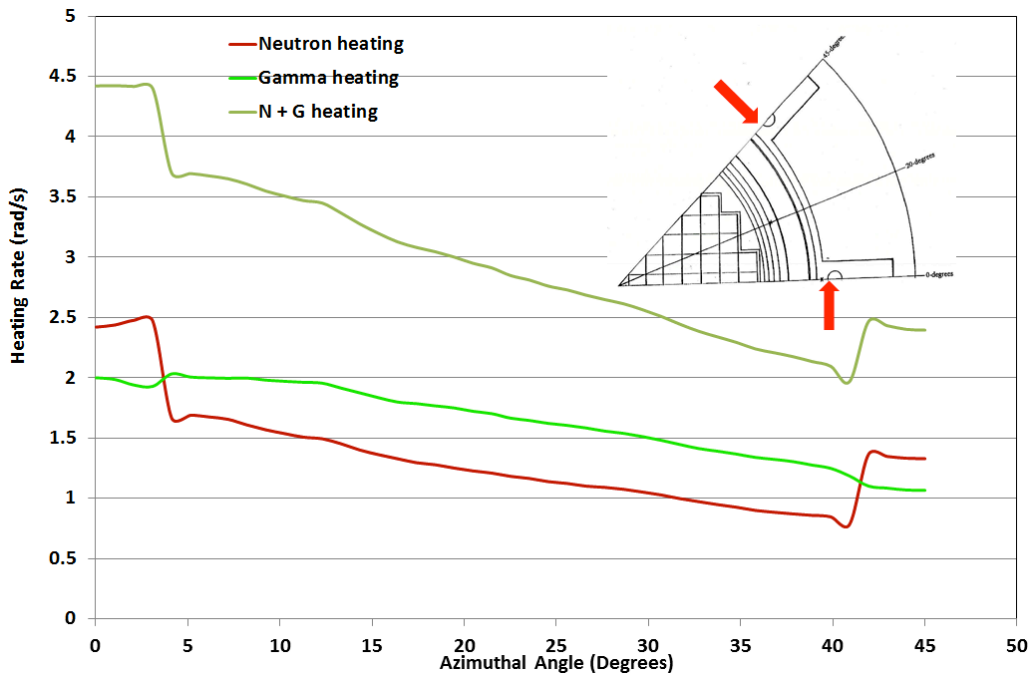


Fig. 7 Azimuthal variation of neutron and gamma heating rates along the radial arc just inside the cylindrical part of the biological shield (as shown in the insert); 3-loop PWR. The heating rates at angles close to 0 and 45-degrees are calculated in the air.

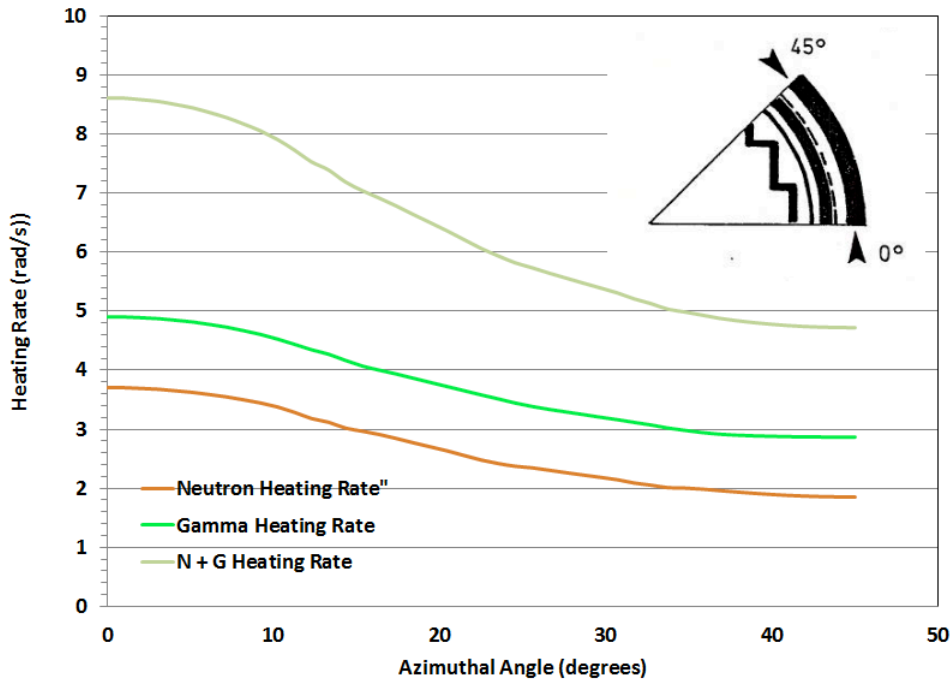


Fig. 8 Azimuthal variation of neutron and gamma heating rates along the radial arc just inside the biological shield (as shown in the insert); 2-loop PWR.

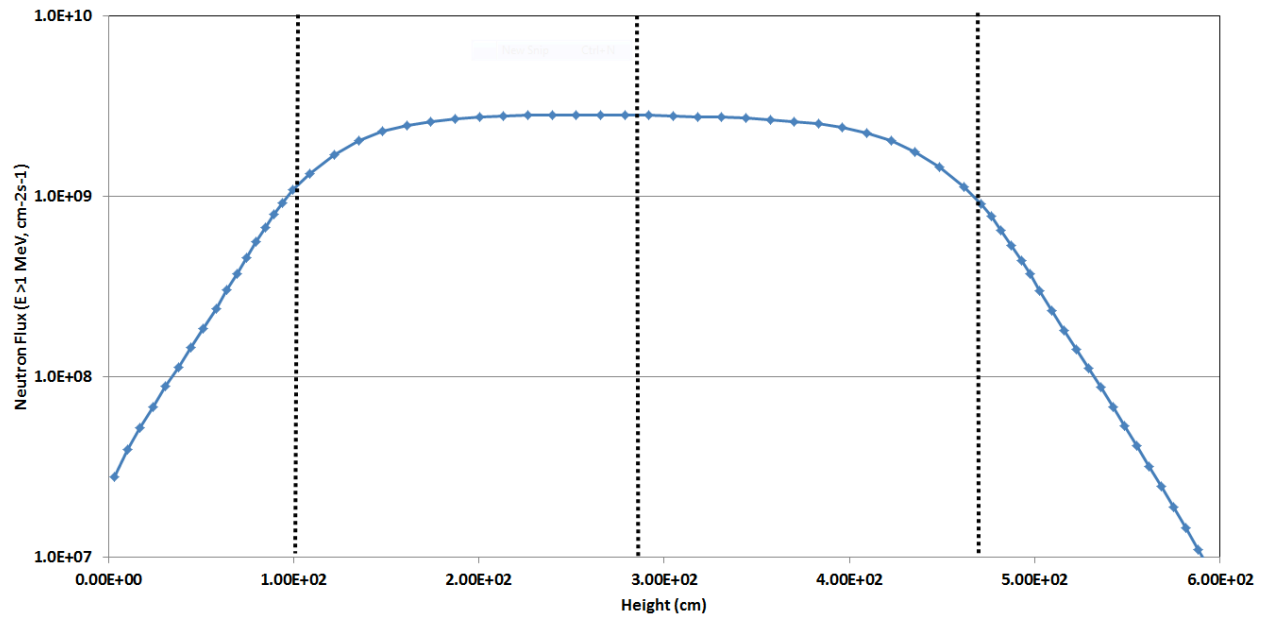


Fig. 9 Variation of fast neutron flux ($E > 1 \text{ MeV}$) with elevation, at the location of the flux maximum in concrete (at $\theta = 0$ -degrees), for the 2-loop PWR. Vertical dotted lines denote the elevation of the bottom, the middle, and the top of the fuel.

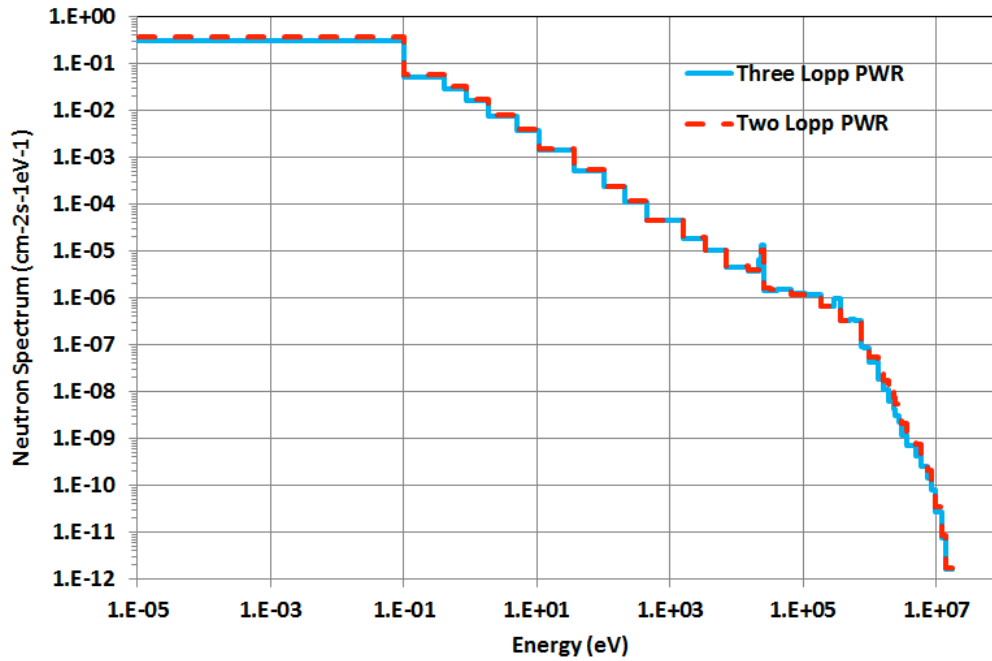


Fig. 10 Comparison of neutron spectra in the cavity of a 3-loop and a 2-loop PWR.

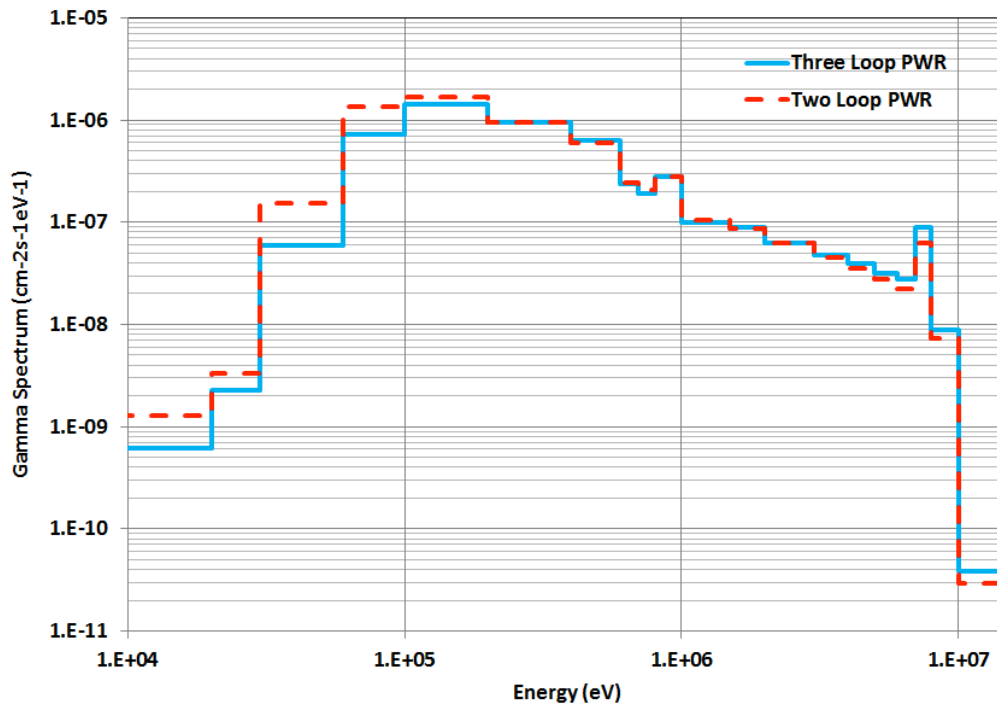


Fig. 11 Comparison of gamma-ray spectra in the cavity of a 3-loop and a 2-loop PWR.

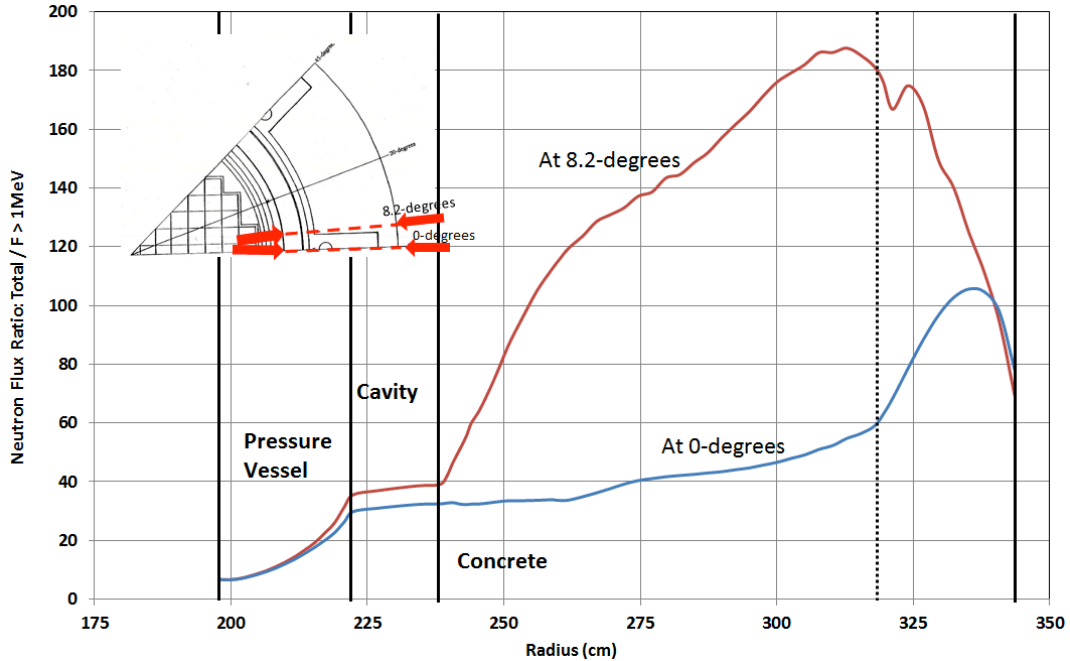


Fig. 12 Ratio of total-to-fast ($E > 1$ MeV) neutron flux versus distance from the core for 3-loop PWR. The insert shows the location of the radial segments plotted on the abscissa. Vertical lines depict the boundaries between PV, cavity, and concrete; the dotted vertical line marks the radial location of the ex-core detector well wall further away from the core.

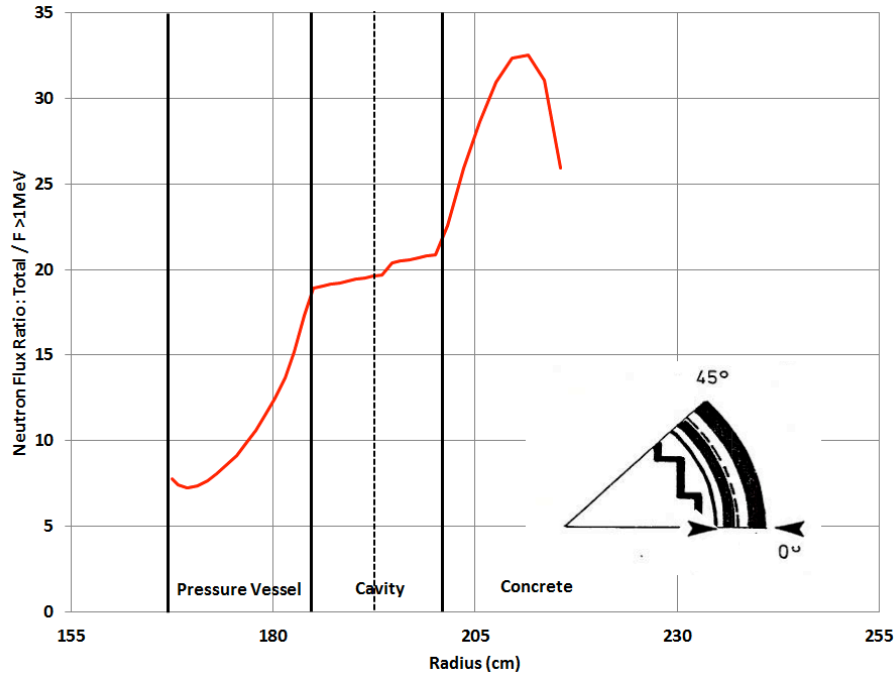


Fig. 13 Ratio of total-to-fast ($E > 1$ MeV) versus distance from the core for 2-loop PWR. The insert shows the location of the radial segment plotted on the abscissa. Vertical lines depict the boundaries between PV, cavity and concrete.